Inorganic Chemistry

pubs.acs.org/IC

Article

Spectroscopic Identification of Trifluorosilylphosphinidene and Isomeric Phosphasilene and Silicon Trifluorophosphine Complex

Guohai Deng, Marc Reimann, Carsten Müller, Yan Lu, Martin Kaupp, and Sebastian Riedel*

Cite This: *Inorg. Chem.* 2024, 63, 7286−7292

Read Online

ACCESS | Metrics & More | Article Recommendations | Supporting Information

ABSTRACT: The perfluorinated silylphosphinidene, F_3SiP, in the triplet ground state is generated by the reaction of laser-ablated silicon atoms with PF_3 in solid neon and argon matrices. The reactions proceed with the initial formation of a silicon trifluorophosphine complex, F_3PSi, in the triplet ground state, and a more stable inserted phosphasilene, $FPSiF_2$, in the singlet ground state upon deposition. The trifluorosilylphosphinidene was formed through F-migration reactions of $FPSiF_2$ and F_3PSi following a two-state mechanism under irradiation with visible light (λ = 470 nm) and full arc light (λ > 220 nm), respectively. High-level quantum-chemical methods support the identification of F_3PSi, $FPSiF_2$, and F_3SiP by matrix-isolation IR spectroscopy.

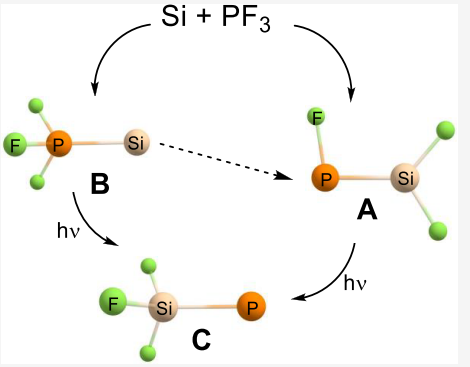

INTRODUCTION

Phosphinidenes (R−P) are highly electron-deficient species that feature monovalent phosphorus analogues of nitrenes (R−N)[1] and carbenes (R−C−R′).[2] As low-valent phosphorus species, they have been widely used in synthetic chemistry as in situ phosphorus agents[3−5] or as ligands in transition metal complexes.[6] Due to their high reactivity and instability, fundamental knowledge about phosphinidenes is mainly achieved by trapping and complexation experiments.[7−11] In contrast to the free nitrenes and carbenes, which have been extensively investigated,[12] only a handful of uncomplexed phosphinidenes have been experimentally identified (Scheme 1). The parent phosphinidene (H−P) (**1**) was observed in the argon matrix following the photolysis of phosphaketene, HPCO.[13] Mesitylphosphinidene (Mes−P) (**2**) and phenylphosphinidene (Ph−P) (**3**) were produced under matrix-isolation conditions through photoelimination of ethylene from the corresponding phosphirane and were spectroscopically characterized.[14−16] Methoxyphosphinidene (CH_3O−P) (**4**) was generated in a cryogenic neon matrix from the photolysis or flash-vacuum pyrolysis of methoxydiazidophosphine, and its isomeric methylphosphinidene oxide was detected.[17] The production of ethynylphosphinidene (HCC−P) (**5**) from the dehydrogenation of phosphapropyne (CH_3CP) via the 1-phosphapropadiene, CH_2=C=PH, and ethynylphosphine, $HCCPH_2$, intermediates through UV-light-induced rearrangement has been reported as well.[18] The simplest silylphosphinidene (H_3Si−P) (**6**) was formed in an argon matrix experiment via reactions of atomic silicon with phosphane.[19] Recently, singlet (phosphino)phosphinidenes (R_2P=P),[20] stable at room temperature, and transient aminophosphinidenes (R_2N=P)[21] have been structurally characterized in the solid state and observed by mass spectrometry, respectively. In addition, the singlet diphosphinylidene H_2P≡P was also prepared and characterized by matrix-isolation IR spectroscopy.[22] All other directly observed free phosphinidenes have triplet electronic ground states.

It should be stressed that no experimental data have been reported on main-group fluorinated phosphinidenes so far. Trifluorosilylphosphinidene, F_3Si−P, the perfluorinated silylphosphinidene, has been theoretically studied several

Scheme 1. Directly Observed Uncomplexed Triplet Phosphinidenes 1−5, as well as Trifluorosilylphosphinidene F_3Si−P and Its Two Isomers, Present Work

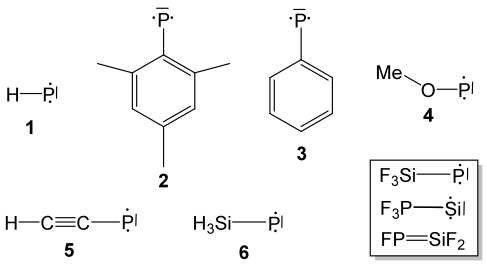

Received: January 11, 2024
Revised: March 25, 2024
Accepted: March 27, 2024
Published: April 9, 2024

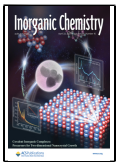

https://doi.org/10.1021/acs.inorgchem.4c00135
Inorg. Chem. 2024, 63, 7286−7292

times.[23,24] It was found that phosphinidene F_3Si-P is the most stable species of four F_3PSi isomers in both the singlet and triplet states due to the strong Si−F bond formation. Previous reports have shown that metal phosphides, $P{\equiv}MF_3$ (Cr, Mo, W, and U),[25,26] and triplet metal phosphinidenes, F_3M-P (Ti, Zr, Hf, and Th),[27,28] can be formed from the reactions of laser-ablated metal atoms with trifluorophosphine. Herein, we report the production and spectroscopic characterization of triplet trifluorosilylphosphinidene via the reaction of laser-ablated silicon atoms with PF_3 in solid neon and argon matrices. We describe that the reactions proceed with the initial formation of a silicon trifluorophosphine complex, F_3PSi, and the more stable inserted isomer $FPSiF_2$ upon deposition. The F_3SiP molecule was synthesized through F-migration reactions of $FPSiF_2$ and F_3PSi under irradiation at visible light (λ = 470 nm) and full arc light (λ > 220 nm), respectively.

RESULTS AND DISCUSSION

The F_3PSi, $FPSiF_2$, and F_3SiP molecules are produced via the reaction of laser-ablated silicon atoms with PF_3 in solid neon and argon matrices. The infrared spectra in the 1000−500 cm^{-1} region obtained by using a 0.05% PF_3/Ne sample are demonstrated in Figure 1. After 30 min sample deposition at 5 K, strong absorption bands of PF_3^- (740.4 and 470.9 cm^{-1})[28] are detected, which decrease on annealing and disappear completely upon full arc light excitation. No obvious PF_2, SiF_2, or SiF_3 absorption bands were observed.[29−31] Besides these known absorption bands, new product absorption bands were detected as well. These absorption bands can be classified into three groups according to their identical chemical behaviors (**A**, **B**, and **C** in Figures 1 and 2). The difference infrared spectra showing the photochemical transformation are given in Figure 2. Similar experiments were repeated by using a 0.2% PF_3/Ar sample. The infrared spectra in the selected region are shown in Figure S1; the corresponding difference infrared spectra are presented in Figure S2. The band positions are summarized in Table 1.

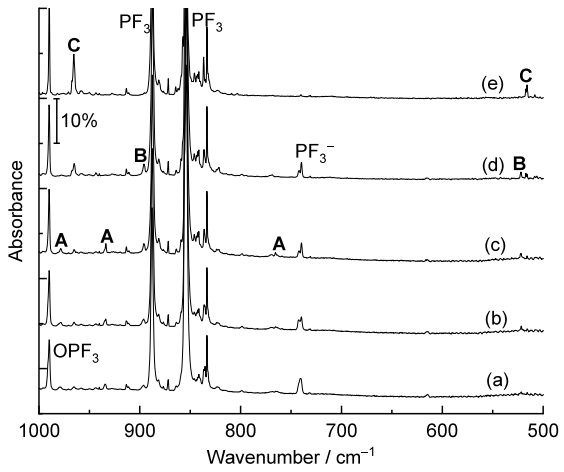

Figure 1. Infrared spectra in the 1000−500 cm^{-1} region from codeposition of laser-ablated Si atoms with 0.05% PF_3 in neon. (a) After 30 min of sample deposition, (b) after annealing to 8 K, (c) after annealing to 10 K, (d) after 10 min of blue LED (λ = 470 nm) light irradiation, and (e) after 10 min of full arc (λ > 220 nm) irradiation. **A**: $FPSiF_2$; **B**: F_3PSi; **C**: F_3SiP.

Product **A** has three absorption bands at 978.5, 933.7, and 765.4 cm^{-1}. They are observed right after deposition and almost do not change when annealing to 10 K but completely disappear under blue LED (λ = 470 nm) light irradiation. Two absorption bands at 891.0 and 520.4 cm^{-1} are observed for product **B**. Both increase slightly under blue LED (λ = 470 nm) light irradiation but disappear upon full arc (λ > 220 nm) irradiation. Product **C** has two absorption bands at 965.5 and 516.0 cm^{-1}. These absorption bands almost do not change upon annealing but remarkably increase under blue LED (λ = 470 nm) light and full arc (λ > 220 nm) irradiation at the expense of the absorption bands of products **A** and **B**, respectively. The product absorption bands in the argon matrix are located at 974.2, 933.1, 759.4 cm^{-1} (**A**), 891.0, 520.4 cm^{-1} (**B**), and 959.7, 513.6 cm^{-1} (**C**). All bands are red-shifted to

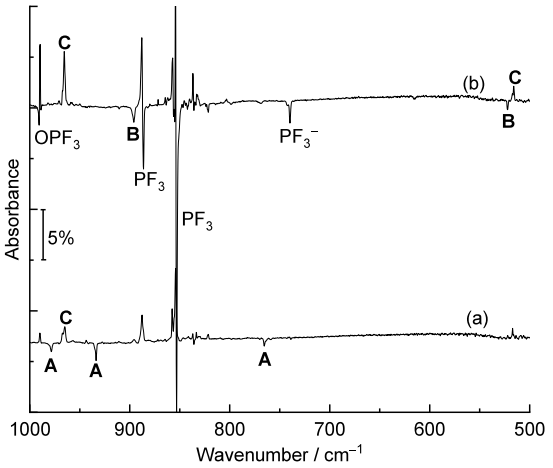

Figure 2. Difference infrared spectra in the 1000−500 cm^{-1} region from codeposition of Si atoms with 0.05% PF_3 in solid neon. (a) Spectrum recorded after 10 min of blue LED (λ = 470 nm) light irradiation minus spectrum recorded after 10 K annealing. (b) Spectrum recorded after 10 min of full arc (λ > 220 nm) irradiation minus spectrum recorded after 10 min of blue LED (λ = 470 nm) light irradiation. **A**: $FPSiF_2$; **B**: F_3PSi; **C**: F_3SiP.

Table 1. Experimentally Observed and Calculated IR Frequencies (cm^{-1}) of $FPSiF_2$, F_3PSi, and F_3SiP Molecules (Absorption Bands above 400 cm^{-1} Are Listed)

	observed		calculated	
species	Ne	Ar	CCSD(T*)-F12[a]	modes[b]
$FPSiF_2$ (**A**)	978.5	974.2	977 (195.5)	asym. SiF_2 str.
	933.7	933.1	933 (255.0)	sym. SiF_2 str.
	765.4	759.4	765 (152.0)	P−F str.
	[c]	[c]	521 (0.4)	P−Si str.
F_3PSi (**B**)	895.9	891.0	902 (178.3)[d]	asym. PF_3 str.
	[e]	[e]	886 (402.7)	sym. PF_3 str.
	522.1	520.4	521 (107.5)	P−Si str.
F_3SiP (**C**)	965.5	959.7	965 (1560.0)[d]	asym. SiF_3 str.
	[e]	[e]	855 (248.9)	sym. SiF_3 str.
	516.0	513.6	514 (76.7)	Si−P str.

[a]Anharmonic frequencies calculated at the CCSD(T*)-F12a/aug-cc-pVTZ-F12 level; the complete sets of vibrational frequencies are provided in Supporting Information Table S1. Intensities in parentheses were obtained from HF dipole moments. [b]Assignments based on calculated vibrational displacement vectors. [c]Absorption band not observed due to small intensity. [d]The component of the formally degenerate vibration with higher intensity is given. [e]Absorption band not observed due to overlap with the PF_3 band.

https://doi.org/10.1021/acs.inorgchem.4c00135
Inorg. Chem. 2024, 63, 7286−7292

lower wavenumbers with respect to their positions in the neon matrix due to the larger polarizability of the argon atom.

Considering the previously reported reactions of silicon atoms with PH_3 to form the H_3PSi, H_2PSiH, $HPSiH_2$, and H_3SiP molecules,[19] and of transition metal atoms with PF_3 to give PMF_3 complexes,[25−28] four possible isomers F_3PSi, F_2PSiF, $FPSiF_2$, and F_3SiP in the electronic singlet and triplet states were studied computationally at the CCSD(T*)-F12a/aug-cc-pVTZ-F12 level.

Products **A** and **B** can be assigned to the phosphasilene isomer, $FPSiF_2$, and the silicon trifluorophosphine isomer, F_3PSi, respectively, by comparison with the computed IR spectra (Table 1 and Table S1). For product **A**, the first two absorption bands belong to antisymmetric and symmetric stretching vibration modes of the SiF_2 moiety. The two frequencies are very close to that of $F_2Si{=}S$ (996, 969 cm^{-1}, Ar matrix)[32] but lower than that in SiF_2 (864.6, 851.0 cm^{-1}, Ne matrix).[30] The band at 765.4 cm^{-1} can be attributed to the P−F stretching vibration, which is red-shifted compared to FP═S (791.4 cm^{-1}, Ar matrix),[33] FP═O (811.4 cm^{-1}, Ar matrix),[34] and FP═NF (826.5 cm^{-1}, Ar matrix).[35] The band positions are in excellent agreement with the computed anharmonic IR frequencies at 977, 933, and 765 cm^{-1} for the singlet $FPSiF_2$ molecule. The predicted P−Si stretching vibration at 521 cm^{-1} is too weak to be observed experimentally.

For product **B**, the absorption band at 895.9 cm^{-1} belongs to the antisymmetric vibration mode of PF_3. This position is very close to the bands of trifluorphosphine and lower than those of transition metal trifluorophosphine complexes.[36] The P−Si stretching vibration occurs at 522.1 cm^{-1} as a weak absorption band. The band position is slightly blue-shifted compared to F_3SiPH_2 (514 cm^{-1}, gas phase).[37] The calculated anharmonic IR frequencies at 902 and 521 cm^{-1} of triplet silicon trifluorophores match the experimental values very well. The PF_3 symmetric stretching vibration was predicted at 886 cm^{-1} as a strong absorption band and could not be observed due to the overlap with the respective band of PF_3. The other computed vibrations of $FPSiF_2$ and F_3PSi are outside the present mid-IR spectral range (4000−450 cm^{-1}).

Experimentally, **C** is produced under the irradiation of products $FPSiF_2$ (**A**) and F_3PSi (**B**). The reactive intermediates generally rearrange to more stable structural isomers or decompose to stable products upon photolysis. In this case, the absence of FP/SiF_2 and P/SiF_3 species among the photolysis products indicates that the P−Si bond in both products was not cleaved when the matrix samples were subjected to light irradiation. This is in accordance with the large P−Si bond dissociation energies of $FPSiF_2$ (33.6 kcal mol^{-1}, CCSD(T*)-F12a/aug-cc-pVTZ-F12) and F_3SiP (68.3 kcal mol^{-1}). Therefore, it is very likely that F-migration happens in matrix-isolated $FPSiF_2$ (**A**) and F_3PSi (**B**) under irradiation conditions. Accordingly, species **C** is safely assigned to the triplet trifluorosilylphosphinidene, F_3SiP, the most stable isomer of F_3PSi. Its predicted vibrational frequencies (Table 1) are in excellent agreement with the detected IR spectra. The SiF_3 antisymmetric stretching mode appears at 965.6 cm^{-1}, which is very close to those of SiF_3 (958.6 cm^{-1}, Ne-matrix)[30] and F_3SiPH_2 (970 cm^{-1}, gas phase).[37] The weak band at 516.0 cm^{-1} is assigned to the Si−P stretching vibration mode, which is blue-shifted to 522.1 cm^{-1} in the F_3PSi complex. However, the computed SiF_3 symmetric vibration at 855 cm^{-1} is not detected due to its overlap with the PF_3 bands in this region. The calculated vibrational frequencies of the proposed isomer F_2PSiF (see Table S1) do not match any experimentally observed IR bands. As the agreement between theory and experiment is excellent for the other isomers, we conclude that no significant amount of F_2PSiF is present at any given time.

The relative energies and structures of F_3PSi isomers **A**, **B**, and **C** determined by ab initio calculations (CCSD(T*)-F12a/aug-cc-pVTZ-F12) are shown in Figure 3. The $FPSiF_2$ (**A**) species was predicted to have a singlet ground state with a planar structure. The calculated Si−P bond length is 2.104 Å, which is close to the value (2.094 Å) determined by X-ray crystallography on phosphasilenes, but slightly longer than those of HPSi (2.045 Å)[38] and $HPSiH_2$ (2.084 Å).[19] The analysis using the AdNDP method[39] on $FPSiF_2$ shows one Si−P σ bond and one Si−P π bond (Figure S3), suggesting the Si−P double bonding character. The calculated Wiberg bond index for the Si−P bond is 1.71, consistent with the AdNDP results. Still, the Si−P bond in $FPSiF_2$ is weaker than the formal single bond in F_3SiP (see above). NBO[40] analysis suggests that this is due to a significant population of the Si−P π^* bond due to negative hyperconjugation.

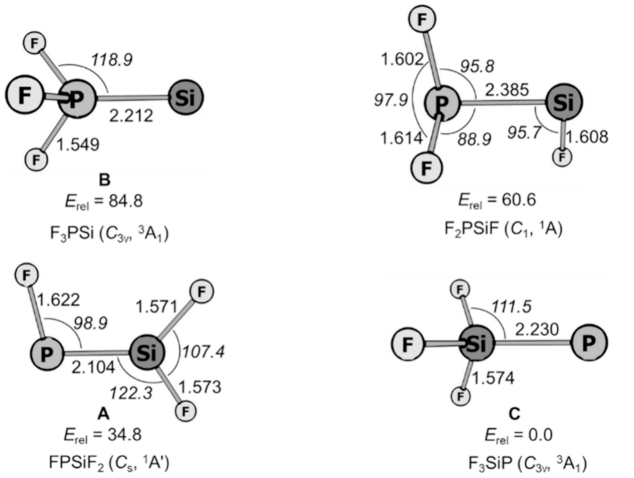

Figure 3. Calculated structures (bond lengths in Ångstrom and bond angles in degrees) and relative energies (kcal mol^{-1}) of four F_3PSi isomers at the CCSD(T*)-F12a/aug-cc-pVTZ-F12 level of theory.

Silicon trifluorophosphine complex **B**, which has not been discussed in earlier theoretical studies, possesses, according to calculations and experiments, a triplet ground state and C_{3v} symmetry. The energetically higher-lying singlet silicon trifluorophosphine has C_1 symmetry and lies 15.2 kcal mol^{-1} above **B**. The computed Si−P bond length (2.212 Å) is larger than in $FPSiF_2$ (2.119 Å) but shorter than in the H-analogue H_3PSi (2.356 Å).[19]

Similar to other phosphinidenes, such as HP,[13] C_6H_5P,[14] CH_3OP,[17] and H_3SiP,[19] which have been characterized by a triplet ground state, the trifluorosilylphosphinidene (**C**) is predicted to have a $^3A_1$ ground state with C_{3v} symmetry. The calculated Si−P bond length is 2.230 Å, which is larger than the values of $FPSiF_2$ (2.119 Å) but close to that of the F_3PSi (2.250 Å) complex, calculated at the same level of theory. Si−P multiple bonding is absent. The calculated singlet−triplet energy gap $\Delta(E_{ST})$ of trifluorosilylphosphinidene is 25.0 kcal mol^{-1}. As the most stable isomer of F_3PSi, the triplet trifluorosilylphosphinidene, F_3SiP (**C**), lies −34.8, −60.6, and −84.8 kcal mol^{-1} below $FPSiF_2$ (**A**), F_2PSiF, and F_3PSi (**B**), respectively.

https://doi.org/10.1021/acs.inorgchem.4c00135
Inorg. Chem. 2024, 63, 7286−7292

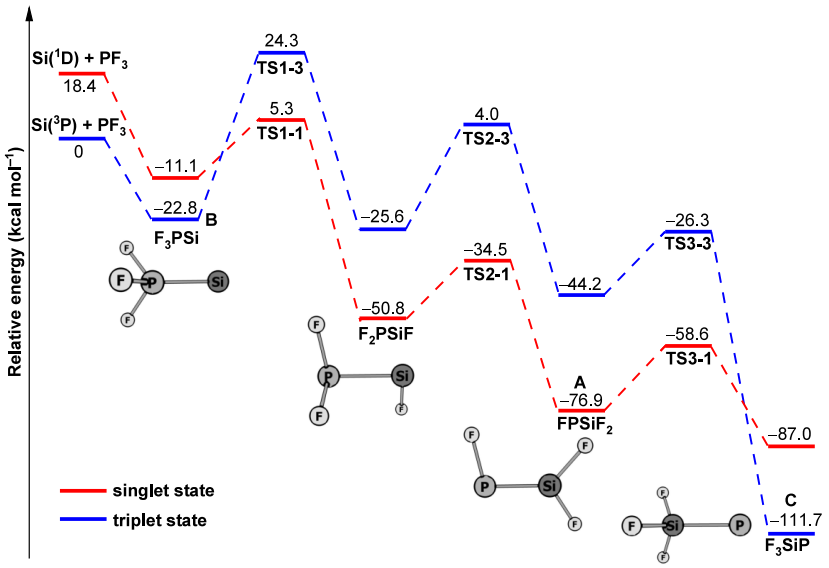

Figure 4. Potential energy profile along the Si + PF_3 reaction path calculated at the CCSD(T*)-F12a/aug-cc-pVTZ-F12//B3LYP/aug-cc-pVTZ level. Energies are given in kcal mol^{-1} relative to the reactants Si(^{3}P) and PF_3.

To unravel the reaction mechanism, the potential energy profile for the reaction of silicon atoms with PF_3 was calculated in both singlet and triplet states at the CCSD(T*)-F12a/aug-cc-pVTZ-F12//B3LYP/aug-cc-pVTZ level. The results are summarized in Figure 4. The structures of the corresponding intermediates and transition states are displayed in Figure S4. Similar to the reaction of a silicon atom with PH_3,[19] the first step of the formation of F_3PSi, starting from a Si atom and trifluorophosphine, is predicted to be exothermic and barrier-free.

If the initial silicon atom has a triplet spin state, we suspect the formation of product **B**. As further barriers on the triplet surface are high, we expect no further reactions at this point. A singlet Si should lead to the formation of singlet F_3PSi, which then reacts thermally to product **A** by fluorine transfer. The intermediately formed F_2PSiF is not isolated as both barriers (TS1−1 and TS2−1) in the process are of similar height. Inspection of the D_1 diagnostics[41] for the CCSD wave functions of the singlet species shows unsuspicious values between 0.01 and 0.05 for every species but the second transition state (TS2−1). For the latter, D_1 surpasses 0.20, indicating a stronger multireference character. This can be rationalized by the fact that $FPSiF_2$ (product **A**) contains a Si−P double bond, while F_2PSiF does not. The transition state between the two is therefore an intermediate between a Si−P single and double bond, giving rise to the importance of at least two different configurations, thereby suggesting a multireference character. As this will give rise to correlation-energy contributions of TS2−1 beyond what is captured at the CCSD(T*)-F12a level, the calculated barrier shown in Figure 4 is an upper bound. Additional calculations with a cc-pVDZ basis set suggest a further lowering of the barrier at TS2−1 compared to that at CCSD(T) by 2 kcal/mol when applying the higher CCSDT(Q) level. The effect on the other barriers is about one order of magnitude smaller. Possibly, further reductions may be expected at levels with even more static correlation. In any case, this barrier is significantly smaller than those at either TS1−1 or at TS3−1. Keeping in mind that energy dissipation in an Ar matrix is much smaller than for reactions in solution yet significant compared to a gas-phase reaction,[42] this is suggested to explain the sole formation of **A** in the thermal reaction. That is, we have to assume that upon formation of **A**, energy dissipation is already so large that the last, higher barrier at TS3−1 cannot be overcome thermally. The computed result is consistent with our experimental observation that only very little product **A** is formed overall.

STEOM-CCSD/aug-cc-pVTZ calculations find a (formally spin-forbidden) singlet−triplet excitation for product **A** at around 465 nm. The formed triplet state can then cross TS3 on the triplet surface and relax to give the final product **C**. This explains the experimentally observed transition from **A** to **C** upon irradiation with blue light. At the same level, the first triplet−triplet excitation of **B** is found only at 390 nm with several more excitations present below 220 nm. Upon irradiation with full arc light, several excited-state pathways will therefore be accessible, allowing for the formation of thermodynamically stable product **C**.

CONCLUSIONS

In conclusion, we report the reactions of laser-ablated silicon atoms and PF_3 forming phosphasilene $FPSiF_2$ (**A**) and silicon trifluorophosphine complex F_3PSi (**B**) in solid neon and argon matrices. The phosphasilene molecule has an electronic singlet ground state, while the silicon trifluorophosphine complex has a triplet ground state. The $FPSiF_2$ (**A**) and F_3PSi (**B**) molecules rearrange to the more stable trifluorosilylphosphinidene F_3SiP (**C**) molecule by one- and three-fluorine atom migration under irradiation at visible light (λ = 470 nm) and full arc light (λ > 220 nm), respectively. The latter molecule is identified to have a triplet electronic ground state.

EXPERIMENTAL AND COMPUTATIONAL DETAILS

The experimental method for matrix-isolation infrared spectroscopy has been described in more detail in our previous works.[43] Briefly, the 1064 nm fundamental of a Nd:YAG laser (Continuum, Minilite II, 10 Hz repetition rate with 10 ns pulse width) with a pulse energy of up to 50−60 mJ cm^{-2} was used to ablate a rotating silicon target (abcr, 99.999%) to form Si atoms. The produced Si atoms were codeposited with PF_3 (abcr, 99%) (0.05%) in excess of neon (0.2% in argon) onto a gold-plated mirror cooled to 4K using a closed-cycle helium

https://doi.org/10.1021/acs.inorgchem.4c00135
Inorg. Chem. 2024, 63, 7286−7292

refrigerator. After 30 min of sample deposition, infrared spectra were recorded on a Bruker Vertex 80 spectrometer at 0.5 cm^{-1} resolution in the region between 4000 and 450 cm^{-1} using a liquid nitrogen-cooled mercury cadmium telluride (MCT) detector. The matrix samples were subjected to irradiation with visible light using a LED light (Oslon 80 4+ PowerStar Circular 4 LED Arrays: $\lambda = 470 \pm 20$ nm) and a medium-pressure mercury arc streetlamp ($\lambda > 220$). No uncommon hazards are noted.

Density functional theory (DFT) calculations were carried out using the Gaussian 16 program package.[44] The hybrid functional B3LYP[45−48] was applied in our calculations to obtain molecular structures of minima and transition states. All stationary points were characterized by the appropriate number of imaginary frequencies. All transition states were further analyzed using an intrinsic reaction coordinate calculation and were confirmed to connect the correct minima of the potential energy surface.

The Coupled Cluster calculations with Single, Double, and perturbative Triple substitutions CCSD(T) were carried out in the closed-shell (RHF-CCSD(T)) and partially spin-restricted open-shell (RHF-RCCSD(T)) formalism using default frozen core settings as implemented in the Molpro2022 software package.[49] To approach the basis set limit, explicitly correlated calculations were performed using the F12a approximation.[50,51] Explicit correlation effects on the perturbative triples were estimated by scaling the (T) contribution as

$$\Delta E^{\mathrm{corr}}{}_{(T^*)} = \Delta E^{\mathrm{corr}}{}_{(T)} \times \Delta E^{\mathrm{corr}}{}_{(\mathrm{MP2-F12})} / \Delta E^{\mathrm{corr}}{}_{(\mathrm{MP2})}$$

All calculations were performed using aug-cc-pVTZ-F12 basis sets[52] as well as the respective auxiliary basis sets automatically assigned by the MOLPRO program.

Anharmonic vibrational frequencies were calculated at the VCISDTQ56 level of theory[53,54] allowing up to five excitations within one mode. VCI calculations were performed on a polynomial fit[55] of a multilevel surface[56,57] using CCSD(T*)-F12a/aug-cc-pVDZ-F12 energies for the two-body and CCSD-F12a/aug-cc-pVDZ-F12 energies for the three-body terms. Intensities were computed using dipole moments at the HF level of theory.

Bonding analyses were carried out by using the adaptive natural density partitioning (AdNDP) method. The color-mapped AdNDP isosurface (0.5 au) graphs were rendered by the VMD 1.9.3 program.[58] Additionally, natural-bond orbital (NBO) analyses were used. Optical excitation energies were obtained at the STEOM-CCSD[59,60] level. Calculations were performed using the ORCA program,[61] Version 5.0.2. All calculations employed the RIJCOSX approximation,[62] the aug-cc-pVTZ basis sets,[63] and the appropriate auxiliary basis sets.[64,65] In every case, the first 10 excitation energies were obtained. Additional CCSDT(Q) calculations were performed using the MRCC program package and the cc-pVDZ basis set.[66]

■ ASSOCIATED CONTENT

Supporting Information

The Supporting Information is available free of charge at https://pubs.acs.org/doi/10.1021/acs.inorgchem.4c00135.

Infrared spectra from co-deposition of silicon atoms with PF_3 in argon; difference infrared spectra from co-deposition of Si atoms with PF_3 in argon; AdNDP chemical bonding and nonbonding pattern of $FPSiF_2$; calculated structural parameters of the higher-energy isomers and the transition states; calculated total energies and IR frequencies for various F_3PSi isomers; and the Cartesian coordinates of the studied complexes (PDF)

■ AUTHOR INFORMATION

Corresponding Author

Sebastian Riedel − *Institut für Chemie und Biochemie−Anorganische Chemie, Freie Universität Berlin, Berlin 14195, Germany;* orcid.org/0000-0003-4552-5719; Email: s.riedel@fu-berlin.de

Authors

Guohai Deng − *Institut für Chemie und Biochemie−Anorganische Chemie, Freie Universität Berlin, Berlin 14195, Germany*

Marc Reimann − *Institut für Chemie, Theoretische Chemie/Quantenchemie, Technische Universität Berlin, Berlin 10623, Germany;* orcid.org/0000-0002-3728-2983

Carsten Müller − *Institut für Chemie und Biochemie−Anorganische Chemie, Freie Universität Berlin, Berlin 14195, Germany*

Yan Lu − *Institut für Chemie und Biochemie−Anorganische Chemie, Freie Universität Berlin, Berlin 14195, Germany*

Martin Kaupp − *Institut für Chemie, Theoretische Chemie/Quantenchemie, Technische Universität Berlin, Berlin 10623, Germany;* orcid.org/0000-0003-1582-2819

Complete contact information is available at: https://pubs.acs.org/10.1021/acs.inorgchem.4c00135

Notes

The authors declare no competing financial interest.

■ ACKNOWLEDGMENTS

We gratefully acknowledge the Zentraleinrichtung für Datenverarbeitung (ZEDAT) of the Freie Universität Berlin for the allocation of computing resources. We thank the CRC 1349 (SFB 1349) Fluorine Specific Interactions Project-ID 387284271 for the continuous support. Open access funding is enabled and organized by Projekt DEAL. G.D. thanks the Alexander von Humboldt Foundation (AvH) for a research scholarship.

■ REFERENCES

(1) Dielmann, F.; Back, O.; Henry-Ellinger, M.; Jerabek, P.; Frenking, G.; Bertrand, G. A Crystalline Singlet Phosphinonitrene: A Nitrogen Atom-transfer Agent. *Science* **2012**, *337*, 1526−1528.

(2) Schreiner, P. R.; Reisenauer, H. P.; Pickard, F. C.; Simmonett, A. C.; Allen, W. D.; Mátyus, E.; Császár, A. G. Capture of Hydroxymethylene and Its Fast Ddisappearance Through Tunnelling. *Nature* **2008**, *453*, 906−909.

(3) Hansmann, M. M.; Bertrand, G. Transition-Metal-like Behavior of Main Group Elements: Ligand Exchange at a Phosphinidene. *J. Am. Chem. Soc.* **2016**, *138*, 15885−15888.

(4) Krachko, T.; Bispinghoff, M.; Tondreau, A. M.; Stein, D.; Baker, M.; Ehlers, A. W.; Slootweg, J. C.; Grützmacher, H. Facile Phenylphosphinidene Transfer Reactions from Carbene-Phosphinidene Zinc Complexes. *Angew. Chem., Int. Ed.* **2017**, *56*, 7948−7951.

(5) Kundu, S.; Sinhababu, S.; Luebben, A. V.; Mondal, T.; Koley, D.; Dittrich, B.; Roesky, H. W. Reagent for Introducing Base-Stabilized Phosphorus Atoms into Organic and Inorganic Compounds. *J. Am. Chem. Soc.* **2018**, *140*, 151−154.

(6) Aktaş, H.; Slootweg, J. C.; Lammertsma, K. Nucleophilic Phosphinidene Complexes: Access and Applicability. *Angew. Chem., Int. Ed.* **2010**, *49*, 2102−2113.

(7) Marinetti, A.; Mathey, F.; Fischer, J.; Mitschler, A. Generation and Trapping of Terminal Phosphinidene Complexes. Synthesis and x-ray Crystal Structure of Stable Phosphirene Complexes. *J. Am. Chem. Soc.* **1982**, *104*, 4484−4485.

(8) Partyka, D. V.; Washington, M. P.; Updegraff, J. B.; Woloszynek, R. A.; Protasiewicz, J. D. Synergistic Binding of Both Lewis Acids and Bases to Phosphinidenes. *Angew. Chem., Int. Ed.* **2008**, *47*, 7489−7492.

(9) Doddi, A.; Bockfeld, D.; Bannenberg, T.; Jones, P. G.; Tamm, M. N-Heterocyclic Carbene-Phosphinidyne Transition Metal Complexes. *Angew. Chem., Int. Ed.* **2014**, *53*, 13568−13572.
(10) Fritz, G.; Vaahs, T.; Fleischer, H.; Matern, E. $tBu_2P-P=PbrtBu_2$·LiBr and the formation of tBu_2P-P. *Angew. Chem., Int. Ed. Engl.* **1989**, *28*, 315−316.
(11) Lu, B.; Zeng, X. Phosphinidenes: Fundamental Propertiesand Reactivity. *Chem.—Eur. J.* **2024**, e202303283.
(12) Moss, R. A.; Platz, M. S.; Jones, M. Jr., Eds. *Reactive intermediate chemistry*; Wiley-Interscience, 2004.
(13) Qian, W.; Lu, B.; Tan, G.; Rauhut, G.; Grützmacher, H.; Zeng, X. Vibrational Spectrum and Photochemistry of Phosphaketene HPCO. *Phys. Chem. Chem. Phys.* **2021**, *23*, 19237−19243.
(14) Mardyukov, A.; Niedek, D.; Schreiner, P. R. Preparation and Characterization of Parent Phenylphosphinidene and Its Oxidation to Phenyldioxophosphorane: The Elusive Phosphorus Analogue of Nitrobenzene. *J. Am. Chem. Soc.* **2017**, *139*, 5019−5022.
(15) Bucher, G.; Borst, M. L. G.; Ehlers, A. W.; Lammertsma, K.; Ceola, S.; Huber, M.; Grote, D.; Sander, W. Infrared, UV/Vis, and W-band EPR Spectroscopic Characterization and Photochemistry of Triplet Mesitylphosphinidene. *Angew. Chem., Int. Ed.* **2005**, *44*, 3289−3293.
(16) Akimov, A. V.; Ganushevich, Y. S.; Korchagin, D. V.; Miluykov, V. A.; Misochko, E. Y. The EPR Spectrum of Triplet Mesitylphosphinidene: Reassignment and New Assignment. *Angew. Chem., Int. Ed.* **2017**, *56*, 7944−7947.
(17) Chu, X.; Yang, Y.; Lu, B.; Wu, Z.; Qian, W.; Song, C.; Xu, X.; Abe, M.; Zeng, X. Methoxyphosphinidene and Isomeric Methylphosphinidene Oxide. *J. Am. Chem. Soc.* **2018**, *140*, 13604−13608.
(18) Lawzer, A.-L.; Custer, T.; Guillemin, J.-C.; Kołos, R. An Efficient Photochemical Route Towards Triplet Ethynylphosphinidene, HCCP. *Angew. Chem., Int. Ed.* **2021**, *60*, 6400−6402.
(19) Glatthaar, J.; Maier, G. Reaction of Atomic Silicon with phosphane: A Matrix-pectroscopic Study. *Angew. Chem., Int. Ed.* **2004**, *43*, 1294−1296.
(20) Liu, L.; Ruiz, D. A.; Munz, D.; Bertrand, G. A Singlet Phosphinidene Stable at Room Temperature. *Chem.* **2016**, *1*, 147−153.
(21) Transue, W. J.; Velian, A.; Nava, M.; García-Iriepa, C.; Temprado, M.; Cummins, C. C. Mechanism and Scope of Phosphinidene Transfer from Dibenzo-7-phosphanorbornadiene Compounds. *J. Am. Chem. Soc.* **2017**, *139*, 10822−10831.
(22) Lu, B.; Wang, L.; Jiang, X.; Rauhut, G.; Zeng, X. Spectroscopic Identification of Diphosphene HPPH and Isomeric Diphosphinyldene PPH_2. *Angew. Chem., Int. Ed.* **2023**, *62*, e202217353.
(23) Chaquin, P.; Gherbi, A.; Masure, D.; Sevin, A. A Theoretical Study of Singlet and Triplet Phosphinidenes PAX_3 (A = C, Si; X = H, F) and Their Rearrangement to Phosphaethenes $XPAX_2$. *Comput. Theor. Chem.* **1996**, *369*, 85−92.
(24) Nguyen, M. T.; van Keer, A.; Vanquickenborne, L. G. The Fluorine Effect on the Stability of Phosphaalkenes, Phosphasilenes, Oxophosphane, Thioxophosphane and Their Rearranged Isomers. *J. Organomet. Chem.* **1997**, *529*, 3−14.
(25) Andrews, L.; Wang, X.; Lindh, R.; Roos, B. O.; Marsden, C. J. Simple $N\equiv UF_3$ and $P\equiv UF_3$ Molecules with Triple Bonds to Uranium. *Angew. Chem., Int. Ed.* **2008**, *47*, 5366−5370.
(26) Wang, X.; Andrews, L.; Lindh, R.; Veryazov, V.; Roos, B. O. A Combined Theoretical and Experimental Study of Simple Terminal Group 6 Nitride and Phosphide $N\equiv MX_3$ and $P\equiv MX_3$ Molecules. *J. Phys. Chem. A* **2008**, *112*, 8030−8037.
(27) Wang, X.; Lyon, J. T.; Andrews, L. Formation and Calculations of the Simple Terminal Triplet Pnictinidene Molecules $N\div MF_3$, $P\div MF_3$, and $As\div MF_3$ (M = Ti, Zr, Hf). *Inorg. Chem.* **2009**, *48*, 6297−6302.
(28) Wang, X.; Andrews, L. Infrared Spectra and Density Functional Calculations of Triplet Pnictinidene $N\div ThF_3$, $P\div ThF_3$ and $As\div ThF_3$ molecules. *Dalton Trans.* **2009**, 9260−9265.
(29) Lugez, C. L.; Irikura, K. K.; Jacox, M. E. Experimental and Ab initio Study of The Infrared Spectra of Ionic Species Derived from PF_5, PF_3, and F_3PO and Trapped in Solid Neon. *J. Chem. Phys.* **1998**, *108*, 8381−8393.
(30) Hastie, J. W.; Hauge, R. H.; Margrave, J. L. Infrared Spectra of Silicon Difluroide in Neon and Argon Matrixes. *J. Am. Chem. Soc.* **1969**, *91*, 2536−2538.
(31) Jacox, M. E.; Irikura, K. K.; Thompson, W. E. Matrix Isolation Study of the Interaction of Excited Neon Atoms with SiF_4: Infrared Spectra of SiF_3^+ and SiF_3^-. *J. Chem. Phys.* **1995**, *103*, 5308−5314.
(32) Beckers, H.; Breidung, J.; Bürger, H.; Köppe, R.; Kötting, C.; Sander, W.; Schnöckel, H.; Thiel, W. Difluorosilanethione $F_2Si = S$ by Flash Vacuum Thermolysis of $(F_3Si)_2S$ and by Reaction of SiS with F_2−Matrix Studies and Ab initio Calculations. *Eur. J. Inorg. Chem.* **1999**, *1999*, 2013−2019.
(33) Beckers, H.; Bogey, M.; Breidung, J.; Bürger, H.; Dre′an, P.; Paplewski, P.; Thiel, W.; Walters, A. FP=S in the Gas-phase: Detection by Rotationally Resolved Infrared and Millimetre-wave Spectra Assisted by Ab-initio Calculations. *Phys. Chem. Chem. Phys.* **2000**, *2*, 2467−2469.
(34) Ahlrichs, R.; Becherer, R.; Binnewies, M.; Borrmann, H.; Lakenbrink, M.; Schunck, S.; Schnoeckel, H. Formation and Structure of Molecular O=P−F. Mass Spectrometry, Infrared Spectra of the Matrix Isolated Species and Ab initio Calculations. *J. Am. Chem. Soc.* **1986**, *108*, 7905−7911.
(35) Zeng, X.; Beckers, H.; Willner, H. Difluoro- λ^5-phosphinonitrile $F_2P\equiv N$: Matrix Isolation and Photoisomerization into FP=NF. *Angew. Chem., Int. Ed.* **2009**, *48*, 4828−4831.
(36) Kruck, T. Trifluorophosphine Complexes of Transition Metals. *Angew. Chem., Int. Ed.* **1967**, *6*, 53−67.
(37) Fritz, G.; Schäfer, H.; Demuth, R.; Grobe, J. Das F_3SiPH_2. *Z. Anorg. Allg. Chem.* **1974**, *407*, 287−294.
(38) Lattanzi, V.; Thorwirth, S.; Halfen, D. T.; Mück, L. A.; Ziurys, L. M.; Thaddeus, P.; Gauss, J.; McCarthy, M. C. Bonding in the Heavy Analogue of Hydrogen Cyanide: The Curious Case of Bridged HPSi. *Angew. Chem., Int. Ed.* **2010**, *49*, 5661−5664.
(39) Zubarev, D. Y.; Boldyrev, A. I. Developing Paradigms of Chemical Bonding: Adaptive Natural Density Partitioning. *Phys. Chem. Chem. Phys.* **2008**, *10*, 5207−5217.
(40) Reed, A. E.; Curtiss, L. A.; Weinhold, F. Intermolecular Interactions from A Natural Bond Orbital, Donor-acceptor Viewpoint. *Chem. Rev.* **1988**, *88*, 899−926.
(41) Janssen, C. L.; Nielsen, I. M. B. New Diagnostics for Coupled-cluster and Møller-Plesset Perturbation Theory. *Chem. Phys. Lett.* **1998**, *290*, 423−430.
(42) Feldman, V.; Sukhov, F.; Orlov, A.; Tyulpina, I. Stabilisation and Reactions of Aliphatic Radical Cations Produced by Fast Electron Irradiation in Solid Argon Matrices. *Phys. Chem. Chem. Phys.* **2003**, *5*, 1769−1774.
(43) Schlöder, T.; Vent-Schmidt, T.; Riedel, S. A Matrix-Isolation and Quantum-Chemical Investigation of FeF_4. *Angew. Chem., Int. Ed.* **2012**, *51*, 12063−12067.
(44) Frisch, M. J.; Trucks, G. W.; Schlegel, H. B.; Scuseria, G. E.; Robb, M. A.; Cheeseman, J. R.; Scalmani, G.; Barone, V.; Petersson, G. A.; Nakatsuji, H.; Li, X.; Caricato, M.; Marenich, A. V.; Bloino, J.; Janesko, B. G.; Gomperts, R.; Mennucci, B.; Hratchian, H. P.; Ortiz, J. V.; Izmaylov, A. F.; Sonnenberg, J. L.; Williams-Young, D.; Ding, F.; Lipparini, F.; Egidi, F.; Goings, J.; Peng, B.; Petrone, A.; Henderson, T.; Ranasinghe, D.; Zakrzewski, V. G.; Gao, J.; Rega, N.; Zheng, G.; Liang, W.; Hada, M.; Ehara, M.; Toyota, K.; Fukuda, R.; Hasegawa, J.; Ishida, M.; Nakajima, T.; Honda, Y.; Kitao, O.; Nakai, H.; Vreven, T.; Throssell, K.; Montgomery, J. A., Jr.; Peralta, J. E.; Ogliaro, F.; Bearpark, M. J.; Heyd, J. J.; Brothers, E. N.; Kudin, K. N.; Staroverov, V. N.; Keith, T. A.; Kobayashi, R.; Normand, J.; Raghavachari, K.; Rendell, A. P.; Burant, J. C.; Iyengar, S. S.; Tomasi, J.; Cossi, M.; Millam, J. M.; Klene, M.; Adamo, C.; Cammi, R.; Ochterski, J. W.; Martin, R. L.; Morokuma, K.; Farkas, O.; Foresman, J. B.; Fox, D. J. *Gaussian 16*, revision C.01; Gaussian, Inc.: Wallingford, CT, 2016.
(45) Vosko, S. H.; Wilk, L.; Nusair, M. Accurate Spin-dependent Electron Liquid Correlation Energies for Local Spin Density Calculations: a Critical Analysis. *Can. J. Phys.* **1980**, *58*, 1200−1211.

https://doi.org/10.1021/acs.inorgchem.4c00135
Inorg. Chem. 2024, 63, 7286−7292

(46) Lee, C.; Yang, W.; Parr, R. G. Development of the Colle-Salvetti Correlation-energy Formula into a Functional of the Electron Density. *Phys. Rev. B* **1988**, *37*, 785−789.
(47) Becke, A. D. Density-functional Thermochemistry. III. The Role of Exact Exchange. *J. Chem. Phys.* **1993**, *98*, 5648−5652.
(48) Stephens, P. J.; Devlin, F. J.; Chabalowski, C. F.; Frisch, M. J. Ab Initio Calculation of Vibrational Absorption and Circular Dichroism Spectra Using Density Functional Force Fields. *J. Phys. Chem.* **1994**, *98*, 11623−11627.
(49) Werner, H.-J.; Knowles, P. J.; Celani, P.; Györffy, W.; Hesselmann, A.; Kats, D.; Knizia, G.; Köhn, A.; Korona, T.; Kreplin, D.; Lindh, R.; Ma, Q.; Manby, F. R.; Mitrushenkov, A.; Rauhut, G.; Schütz, M.; Shamasundar, K. R.; Adler, T. B.; Amos, R. D.; Bennie, S. J.; Bernhardsson, A.; Berning, A.; Black, J. A.; Bygrave, P. J.; Cimiraglia, R.; Cooper, D. L.; Coughtrie, D.; Deegan, M. J. O.; Dobbyn, A. J.; Doll, K.; Dornbach, M.; Eckert, F.; Erfort, S.; Goll, E.; Hampel, C.; Hetzer, G.; Hill, J. G.; Hodges, M.; Hrenar, T.; Jansen, G.; Köppl, C.; Kollmar, C.; Lee, S. J. R.; Liu, Y.; Lloyd, A. W.; Mata, R. A.; May, A. J.; Mussard, B.; McNicholas, S. J.; Meyer, W.; Miller, III, T. F.; Mura, M. E.; Nicklass, A.; O'Neill, D. P.; Palmieri, P.; Peng, D.; Peterson, K. A.; Pflüger, K.; Pitzer, R.; Polyak, I.; Reiher, M.; Richardson, J. O.; Robinson, J. B.; Schröder, B.; Schwilk, M.; Shiozaki, T.; Sibaev, M.; Stoll, H.; Stone, A. J.; Tarroni, R.; Thorsteinsson, T.; Toulouse, J.; Wang, M.; Welborn, M.; Ziegler, B. *MOLPRO*, version 2022.2, a package of ab initio programs; Cardiff, U. K. 2022, see https://www.MOLPRO.net.
(50) Knizia, G.; Adler, T. B.; Werner, H.-J. Simplified CCSD(T)-F12 Methods: Theory and Benchmarks. *J. Chem. Phys.* **2009**, *130*, 54104.
(51) Adler, T. B.; Knizia, G.; Werner, H.-J. A Simple and Efficient CCSD(T)-F12 Approximation. *J. Chem. Phys.* **2007**, *127*, 221106.
(52) Sylvetsky, N.; Kesharwani, M. K.; Martin, J. M. L. The aug-cc-pVnZ-F12 Basis Set Family: Correlation Consistent Basis Sets for Explicitly Correlated Benchmark Calculations on Anions and Noncovalent Complexes. *J. Chem. Phys.* **2017**, *147*, 134106.
(53) Mathea, T.; Petrenko, T.; Rauhut, G. Advances in Vibrational Configuration Interaction Theory − part 2: Fast Screening of the Correlation Space. *J. Comput. Chem.* **2022**, *43*, 6−18.
(54) Mathea, T.; Rauhut, G. Advances in Vibrational Configuration Interaction Theory - part 1: Efficient Calculation of Vibrational Aangular Momentum Terms. *J. Comput. Chem.* **2021**, *42*, 2321−2333.
(55) Ziegler, B.; Rauhut, G. Efficient Generation of Sum-of-products Representations of High-dimensional Potential Energy Surfaces Based on Multimode Expansions. *J. Chem. Phys.* **2016**, *144*, 114114.
(56) Ziegler, B.; Rauhut, G. Rigorous Use of Symmetry within the Construction of Multidimensional Potential Energy Surfaces. *J. Chem. Phys.* **2018**, *149*, 164110.
(57) Rauhut, G. Efficient Calculation of Potential Energy Surfaces for the Generation of Vibrational Wave Functions. *J. Chem. Phys.* **2004**, *121*, 9313−9322.
(58) Humphrey, W.; Dalke, A.; Schulten, K. VMD:Visual Molecular Dynamics. *J. Mol. Graphics* **1996**, *14*, 33−38.
(59) Huntington, L. M. J.; Krupička, M.; Neese, F.; Izsák, R. Similarity Transformed Equation of Motion Coupled-cluster Theory Based on an Unrestricted Hartree-Fock Reference for Applications to High-spin Open-shell Systems. *J. Chem. Phys.* **2017**, *147*, 174104.
(60) Dutta, A. K.; Nooijen, M.; Neese, F.; Izsák, R. Automatic Active Space Selection for the Similarity Transformed Equations of Motion Coupled Cluster Method. *J. Chem. Phys.* **2017**, *146*, 74103.
(61) Neese, F. Software update: The ORCA Program System—Version 5.0. *WIREs Comput. Mol. Sci.* **2022**, *12*, e1606.
(62) Neese, F.; Wennmohs, F.; Hansen, A.; Becker, U. Efficient, Approximate and Parallel Hartree−Fock and Hybrid DFT Calculations. A 'chain-of-spheres' Algorithm for the Hartree−Fock Exchange. *Chem. Phys.* **2009**, *356*, 98−109.
(63) Kendall, R. A.; Dunning, T. H.; Harrison, R. J. Electron Affinities of the First−row Atoms Revisited. Systematic Basis Sets and Wave Functions. *J. Chem. Phys.* **1992**, *96*, 6796−6806.
(64) Weigend, F.; Köhn, A.; Hättig, C. Efficient Use of the Correlation Consistent Basis Sets in Resolution of the Identity MP2 Calculations. *J. Chem. Phys.* **2002**, *116*, 3175−3183.
(65) Weigend, F. A Fully Direct RI-HF Algorithm: Implementation, Optimised Auxiliary Basis Sets, Demonstration of Accuracy and Efficiency. *Phys. Chem. Chem. Phys.* **2002**, *4*, 4285−4291.
(66) Kallay, M.; Nagy, P. G.; Mester, D.; et al. MRCC, a Quantum Chemical Program Suite. See www.mrcc.hu. DOI: DOI: 10.1063/1.5142048.

https://doi.org/10.1021/acs.inorgchem.4c00135
Inorg. Chem. 2024, 63, 7286−7292